Pharmaceutical Research, Vol. 24, No. 11, November 2007 (© 2007)
DOI: 10.1007/s11095-007-9335-z

Research Paper

Micelles of Different Morphologies—Advantages of Worm-like Filomicelles of PEO-PCL in Paclitaxel Delivery

Shenshen Cai,[1] Kandaswamy Vijayan,[1] Debbie Cheng,[1] Eliana M. Lima,[1] and Dennis E. Discher[1,2]

Received April 10, 2007; accepted May 2, 2007; published online June 13, 2007

Purpose. Worm-like and spherical micelles are both prepared here from the same amphiphilic diblock copolymer, poly(ethylene oxide)-*b*-poly (ε-caprolactone) (PEO [5 kDa]–PCL [6.5 kDa]) in order to compare loading and delivery of hydrophobic drugs.
Materials and Methods. Worm-like micelles of this degradable copolymer are nanometers in cross-section and spontaneously assemble to stable lengths of microns, resembling filoviruses in some respects and thus suggesting the moniker 'filomicelles'. The highly flexible worm-like micelles can also be sonicated to generate kinetically stable spherical micelles composed of the same copolymer.
Results. The fission process exploits the finding that the PCL cores are fluid, rather than glassy or crystalline, and core-loading of the hydrophobic anticancer drug delivery, paclitaxel (TAX) shows that the worm-like micelles load and solubilize twice as much drug as spherical micelles. In cytotoxicity tests that compare to the clinically prevalent solubilizer, Cremophor® EL, both micellar carriers are far less toxic, and both types of TAX-loaded micelles also show fivefold greater anticancer activity on A549 human lung cancer cells.
Conclusion. PEO–PCL based worm-like filomicelles appear to be promising pharmaceutical nanocarriers with improved solubilization efficiency and comparable stability to spherical micelles, as well as better safety and efficacy *in vitro* compared to the prevalent Cremophor® EL TAX formulation.

KEY WORDS: lung carcinoma cells; paclitaxel; poly(ε-caprolactone); poly(ethylene oxide); worm-like micelle.

INTRODUCTION

Parenteral delivery of chemotherapeutics is a cornerstone of clinical cancer treatment, but many drugs are hydrophobic and require a solubilizing carrier. Such systems must load and stably retain anticancer drugs and must also have a means to release drugs into cells. Anticancer drug delivery systems have thus far included bioconjugates (1–3), nanoparticles (4,5), liposomes (6,7), polymersomes (8–10), and polymeric micelles composed of amphiphilic block copolymers (11,12), but all of the cited carriers are essentially spherical in shape. Long and flexible "worm-like" micelle carriers made from amphiphilic block copolymers are described here in terms of formulation and *in vitro* delivery, and the findings follow up on recent studies that demonstrate surprisingly persistent circulation and potent anti-tumor activity of worm-like micelles *in vivo* (13).

Paclitaxel (TAX) is a clinically prevalent anticancer agent used against a variety of solid tumors (14–17), and it works by stabilizing microtubules and inhibiting cytoskeleton-mediated processes such as mitosis (18). However, the extremely low water solubility of TAX at 0.3 μg/ml (25°C) (18) or 3–4 μg/ml at 37°C (19) has motivated both covalent modifications to increase solubility (20) as well as loading into various types of carrier systems. As the most common emulsifying agent used in the clinic to solubilize TAX, Cremophor® EL is a complex, viscous mixture composed primarily of hydrophobic glycerolpolyoxyethylene ricinoleates, various fatty acid esters, and ~50% ethanol (21,22), but clinical problems associated with Cremophor EL include low drug stability after dilution in aqueous medium (23) and severe, dose-limiting side effects such as hypersensitivity and cardiotoxicity (20,24,25). There is therefore a need for safer and more effective TAX delivery systems.

Amphiphilic diblock copolymers generally self-assemble in dilute aqueous solution into three basic morphologies: spherical micelles, worm-like micelles, and vesicles. Spherical micelles form spontaneously when the hydrophilic, corona block such as poly(ethylene oxide) (PEO) is the largest block by mass, and these have now been widely studied in bioapplication. Following parental administration, such spheres delay clearance by macrophages of the liver and spleen due to the hydrated corona and also—it has been thought—due to their small size (26). Escape from clearance in principle allows accumulation in tumors, and use of copolymers that are degradable (27,28) or sensitive to temperature or pH can provide mechanisms for controlled drug release (18,24,29). By decreasing the weight fraction of the PEO block to just less than ~50%, hydration and swelling of the corona imparts just enough curvature to the copolymer assembly that worm-like micelles that are microns in length and similar in

[1] Department of Chemical and Biomolecular Engineering, University of Pennsylvania Philadelphia, Pennsylvania, 19104, USA.
[2] To whom correspondence should be addressed. (e-mail: discher@seas.upenn.edu)

diameter to the spheres are the predominant morphology for a variety of diblock copolymers (30,31). Drugs such as TAX and various hydrophobic dyes have now been loaded into these novel carriers (30,32–34), and worm-like micelles *in vivo* persist for up to 1 week in the blood circulation, which appears longer than any other synthetic particle, including stealthy vesicles bearing the same length of PEO chains (13). In some sense, the worm-like micelles are bio-inspired by filoviruses that can also circulate and infect human cells, which is why the micelles are hereafter referred to as filomicelles.

In this study, worm-like filomicelles and spherical micelles were both prepared from the same poly (ethylene oxide)-*b*-poly (ε-caprolactone) (PEO-PCL, denoted OCL) as sketched in Fig. 1a. Drug loading capacities were then directly compared, and show that approximately 2-fold higher TAX loading is possible with worm-like filomicelles. For both systems, TAX release is similarly enhanced at lower pH, which is favorable as cancerous tissues are generally associated with acidic environment (29,35). Compared to Cremophor EL, both polymeric micelle carriers show significantly less cytotoxicity and greater potency in delivering TAX to human lung carcinoma A549 cells. OCL-based worm-like filomicelles thus appear to be a promising new system for drug delivery.

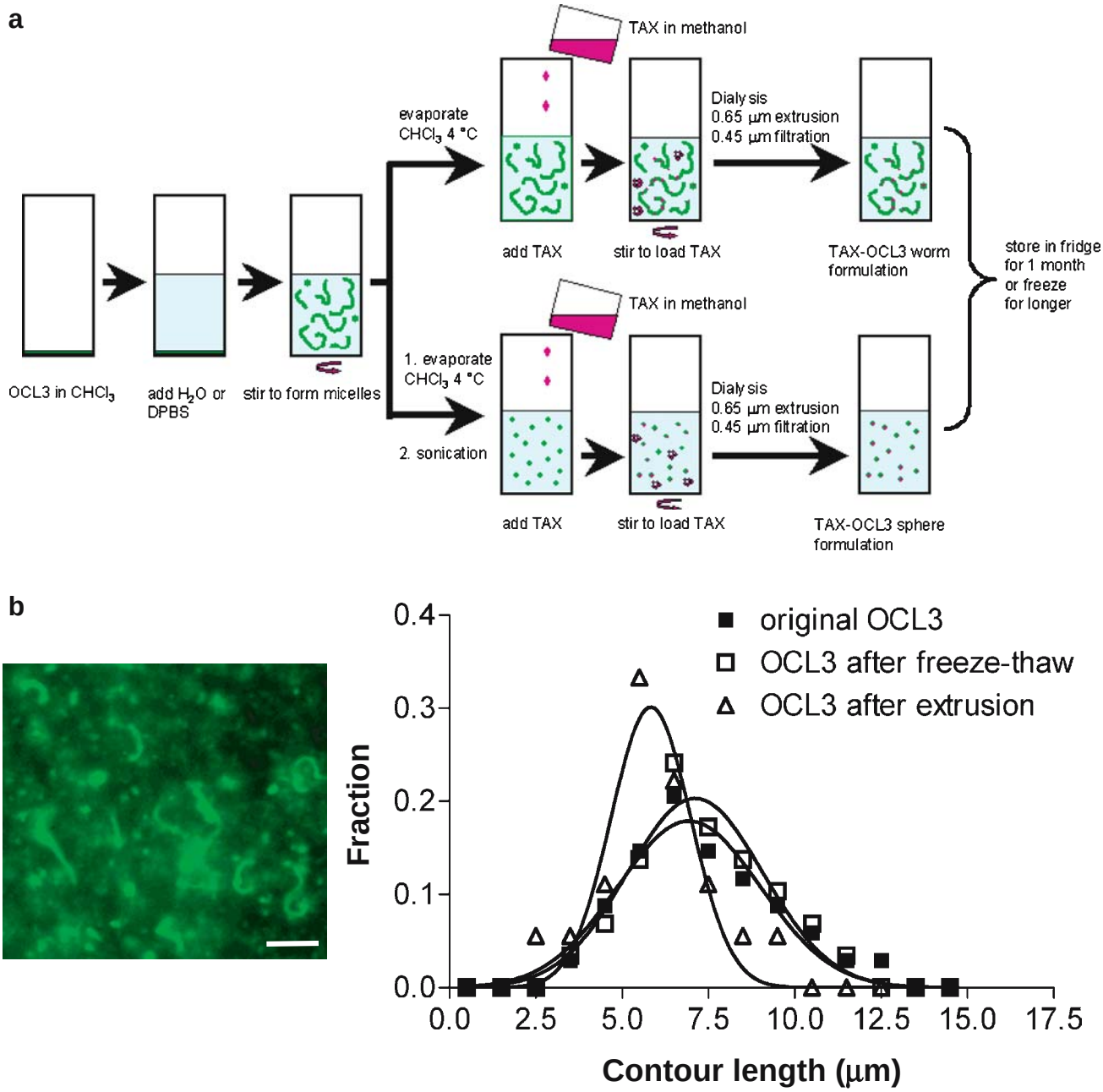

Fig. 1. Preparation of OCL3 polymeric micelles. **a** Scheme of making OCL3 micelles in worm-like and spherical morphologies; **b** visualization of worm-like micelles under fluorescence microscopy (*left*) and the contour length distribution of worm-like micelles, *inset* showing an enlarged worm-like micelle (*right*). *Scale bar* 5 μm.

MATERIALS AND METHODS

Materials

Diblock polymer poly (ethylene oxide)-*b*-poly (ε-caprolactone) (M_n =5,000–6,500, weight fraction of PEO f_{EO}=0.43, polydispersity= 1.3, denoted OCL3) was purchased from Polymersource (Dorval, Canada). Paclitaxel (TAX), docetaxel, Cremophor EL, fluorescent PKH26 dye, Dulbecco's phosphate-buffered saline (DPBS) and methylthiazolyldiphenyl-tetrazolium bromide (MTT) were from Sigma (St. Louis, MO). Human lung carcinoma cells A549 were obtained from ATCC (Manassas, VA). F12 Ham media was purchased from Mediatech (Herndon, VA). All organic solvents were analytical grade from Fisher Scientific.

Preparation of OCL3 Polymeric Micelles by Cosolvent/ Evaporation Method

The preparation of OCL3 polymeric micelles was shown in Fig. 1a. Briefly, 50 μl of 50 mg/ml OCL3 stock solution in chloroform was mixed with 5 ml of water and the mixture was stirred vigorously at room temperature for 1 h. Chloroform was completely removed by evaporation at 4°C for overnight to obtain the final solution containing OCL3 worm-like micelles. Solutions at other concentrations were made by varying the volume of OCL3 stock solution mixed with water. OCL3 spherical micelles were obtained by sonicating the worm-like micelles using Fisher 60 Sonic Dismembrator equipped with Fisher Ultrasonic Converter (Fisher Scientific) for 25 pulses at 1 s/pulse. All solutions containing OCL3 polymeric micelles were stored at 4°C to minimize degradation.

Fluorescence Microscopy and Micelle Morphology Studies

PKH26, which is a rhodamine-based hydrophobic fluorescent dye, was added to OCL3 micelle solutions at about 1 μl/1 mg polymer and vortexed for 10 s. The dye rapidly distributed into the hydrophobic core of the micelles so the morphology of micelles was visualized. Olympus IX71 inverted fluorescence microscope equipped with a 60× objective lens and a Cascade CCD camera was used to observe the micelles. About 25 images were taken for each sample tested and the contour length of worm-like micelles was measured using Image-Pro Plus (MediaCybernetics, Silver Spring, MD).

Dynamic Light Scattering

The average hydrodynamic micelle sizes and size distribution were analyzed by dynamic light scattering (DLS) using Protein Solutions™ Temperature Controlled MicroSampler and Protein Solutions Dynapro™ Titan (Wyatt Technologies, Santa Barbara, CA) at 25°C. The laser wavelength was 782.4 nm and the scattering angle was 90°. Each sample was measured in triplicate.

Crystallinity Analysis

Polycaprolactone is a highly crystalline polymer in bulk. In an attempt to look for crystallization at nano-scale, an alternate protocol was developed that could exploit the melting and annealing of the PCL core. Thus a 10 mg/ml stock solution of OCL3 was prepared in chloroform and 15–20 μl of this stock was added to 1 ml water in a glass vial. The vial was closed, briefly vortexed, and allowed to stand at room temperature for 2 h. Next, the vial was incubated at 60°C with the cap open, for 2 h to evaporate the chloroform in the solution. The vial was then allowed to incubate at 30°C for 4–6 h. Glycerol was added to the worms to make a 50% glycerol solution, which was incubated at −20°C for up to 24 h. The rigidity of OCL3 worms was determined by fluorescence image analysis as described in "Fluorescence Microscopy and Micelle Morphology Studies."

The fluidity of the worm micelle core was estimated by measuring the fluorescence recovery after photobleaching (FRAP) of the PKH26 dye. Briefly, an aperture on the light path is used to selectively overexpose a small section of the worm. The fluorescence recovery in the bleached region is monitored by comparing the fluorescent intensity to that of the Intensity in an unbleached section of the worm.

Paclitaxel (TAX) Encapsulation in OCL3 Micelles

TAX of 50 mg/ml in methanol was added into the micelle solutions to obtain desired spiked TAX/polymer ratios. The mixture was stirred at 25°C for 20 min and transferred to dialysis cassettes (MWCO 10,000, Pierce, Rockford, IL). Dialysis was performed against DPBS (pH 7.4) for 2 h to remove methanol and small residues of dissolved TAX, and the obtained TAX-loaded micelles were separated from insoluble-free TAX aggregates by extrusion through a 10 ml thermobarrel extruder (Northern Lipids, Vancouver, Canada) fitted with 0.65 μm filtering membranes (Millipore, Bedford, MA), and further purified by filtration through 0.45 μm Fischerbrand MCE filter (Fisher Scientific). The preparation of TAX-encapsulated OCL3 micelles is illustrated in Fig. 1a. As an alternative method, TAX was mixed with OCL3 polymer in chloroform solution before micelle formation. The TAX-loaded micelles were then obtained as described in "Preparation of OCL3 Polymeric Micelles by cosolvent/Evaporation Method" followed by dialysis and extrusion.

HPLC Assay Development and Validation

A Waters HPLC system (Waters, Milford, MA) equipped with a 1525 Binary HPLC pump, a symmetry® reverse-phase C_{18} 5.0 μm column (4.6×150 mm), and a 2487 Dual λ absorbance UV detector was used for TAX quantification. A series of 1:2 TAX dilutions in acetonitrile ranging from 0 to 0.25 mg/ml were pre-mixed with equal volume of 0.25 mg/ml docetaxel in acetonitrile as internal standard. The solutions were filtered through 0.45 μm filter followed by injection into HPLC system. A mobile phase of 58% H_2O, 42% acetonitrile at a flow rate of 1 ml/min was applied. TAX was detected and quantified at UV 220 nm. The standard curve by plotting the ratio of AUC of TAX and docetaxel was established, and the linear range, intra-day and inter-day coefficient of variance (CV), lower limit of detection (LLOD), lower limit of quantification (LLOQ), assay accuracy and recovery (by testing with 3, 10, and 40 μg/ml TAX solution using the standard curve) were calculated. To use the validated HPLC assay to determine the TAX loading capacity and efficiency

in OCL3 micelles, TAX-loaded micelles were pre-mixed with equal volume of 0.25 mg/ml docetaxel in acetonitrile, and acetonitrile in equal volume to the mixture was further added, followed by the HPLC analysis using the standard curve described above. TAX loading capacity and efficiency were calculated based on the following expressions:

$$\text{TAX loading capacity} = \frac{\text{mass of TAX encapsulated in micelles}}{\text{mass of OCL3 polymeric micelles}}$$

$$\text{TAX loading efficiency} = \frac{\text{mass of TAX encapsulated in micelles}}{\text{mass of initially added TAX}}$$

Thermal Analysis

Thermal tests of OCL3 micelles were performed by differential scanning calorimetry (DSC) using a Differential Scanning Calorimeter 2920 (TA instruments, New Castle, DE).

TAX-loaded OCL3 worm micelles were lyophilized before the analysis. DSC thermograms of OCL3–TAX mixture (either in bulk before TAX loading or in lyophilized form after TAX loading) and OCL3 alone were then obtained by heating in sealed standard aluminum pans (TA instruments) from 25 to 100°C at a rate of 10°C/min followed by air cool and reheating to 100°C at the same rate.

Micelle Stability and Paclitaxel Release Studies

Both worm-like and spherical micelles (10 mg/ml), either drug-loaded or free, were stored at 4°C for 1 month or subjected to one-time freeze–thawing cycle. Then, the particle size was measured by DLS and the morphology was tested by fluorescent microscopy. TAX-loaded micelles were also examined for drug leakage potentially caused by storage or freeze–thawing cycles by centrifugation at 3,000 rpm for 5 min to precipitate the TAX that may have diffused out. The supernatant was then mixed with acetonitrile and internal standard docetaxel for HPLC analysis.

Further, a dialysis method was employed to evaluate the *in vitro* release of TAX from OCL3 micelles. TAX-loaded worm-like and spherical micelles at a TAX concentration of 40 μg/ml were added to the dialysis cassettes and dialyzed at 37°C against DPBS of pH 6.8 and pH 7.4. At certain time points, the release medium was sampled and fresh DPBS was added to maintain the volume. The sampled medium was lyophilized and redissolved in chloroform. The insoluble buffer salt was removed by filtration. Chloroform was evaporated then and the remaining sample was re-dissolved in acetonitrile and subjected to aforementioned HPLC analysis.

Cytotoxicity Assay

TAX-loaded and drug-free micelles at serial dilutions were prepared per above. For comparison, 12 mg/ml TAX in ethanol was mixed with equal volume of Cremophor® EL followed by sonication for 30 min. The obtained Cremophor EL TAX was diluted with DPBS to obtain desired TAX concentrations.

Human lung-derived carcinoma cells A549 were grown in F12 Ham media supplemented with 10% fetal bovine serum and 100 U/ml penicillin and 100 μg/ml streptamycin at 37°C, 5% CO_2 to 60–70% confluence. A549 cells (50,000 cell/ml) were seeded in 96-well plates at 5,000 cells per well and cultured for 24 h to allow attachment. The medium was then exchanged and 100 μl of different tested formulations (free worm-like and spherical OCL3 micelles, Cremophor EL, free drug, TAX-loaded worm-like and spherical micelles, and Cremophor EL TAX) was added. As control, 100 μl of DPBS was added to cells not exposed to those formulations. After 37°C, 5% CO_2 incubation for 72 h, the media were discarded, and 100 μl/well F12 Ham medium and 11 μl/well of 5 mg/ml MTT solution in DPBS was added. The plates were incubated at 37°C for 3 h and the media were removed again. The intracellular metabolized product MTT formazan was retrieved by addition of 100 μl/well DMSO and incubation at room temperature for 5 min. The plates were read at 550 nm, and the cell viability was calculated as (reading of wells with cells exposed to tested formulations—reading of blank wells)/(reading of wells with cells exposed to DPBS—reading of blank wells).

Data Analysis

All data that require non-linear regression analysis were processed using GraphPad Prism (Version 4.03, GraphPad Software, San Diego, CA). The contour length distribution of OCL3 worm-like micelles was fit by Gaussian distribution, TAX and the carrier cytotoxicity assay on A549 cells was fit by sigmoid dose–response curve equation.

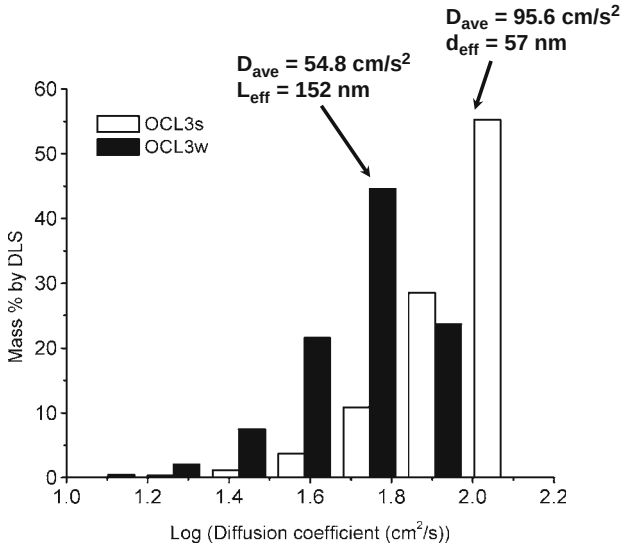

Fig. 2. Size and diffusion analysis of OCL3 micelles. The average diffusion coefficient distribution, and the calculated effective hydrodynamic size (diameter or length) of worm-like (before sonication) and spherical (after sonication) micelles were measured by DLS. The calculation of effective length of worm-like micelles is based on Stokes–Einstein equation: $D=\mathrm{kT}/(2\pi\eta L_{\mathrm{eff}})$ for worms (43) and $D=kT/(3\pi\eta d_{\mathrm{eff}})$ for spheres, where D is the diffusion coefficient, k is the Boltzmann constant (1.38×10^{-23} J/K), T is the temperature (25°C), η is the viscosity of the solution (1.02 mPa·s from DLS), and d_{eff} is the hydrodynamic radius multiplied by 2.

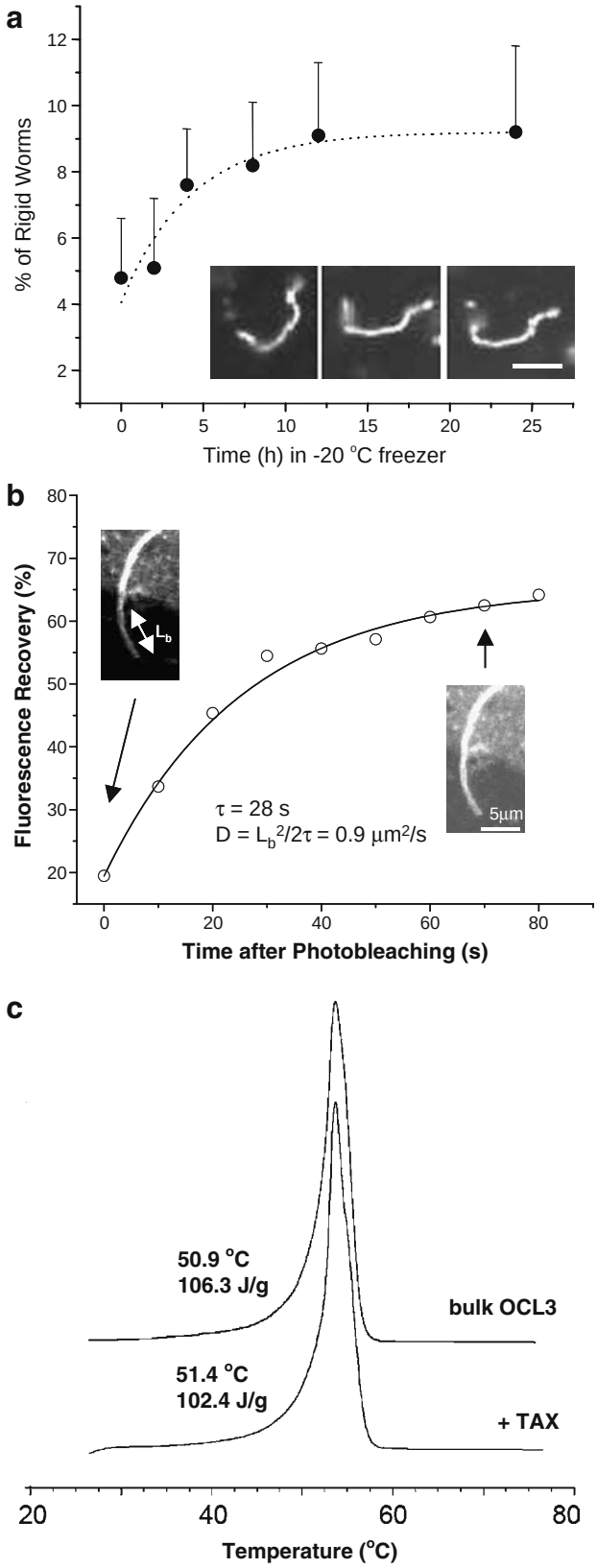

Fig. 3. Thermal and crystallinity analysis of OCL3 micelles. **a** Fluorescence recovery after photobleaching (FRAP) curve on OCL3 worms: A manual aperture in the light path was used to overexpose a small end section of the worm. The intensity in the bleached section was compared to that of a similar length of the worm in the unbleached section to normalize for bleaching during imaging. The FRAP data were fitted to an exponential recovery curve: Recovery % $= A(1 - e^{-t/\tau})$ (where A is the maximum recovery percentage and t is the time for recovery) to obtain an average recovery time constant τ ~28 s. The 1-D diffusivity of the PKH26 dye was calculated from $D = L_b^2/2\tau$ where L_b is the length of the bleached region, and τ is the recovery time constant. D ~0.9 μm²/s. **b** Percentage of rigid OCL3 worm-like micelles with possible crystallized cores over 12 h incubation at −20°C either in a 50% glycerol solution or pure water, after heating to 60°C and cooling to 30°C. The *inset figures* show frames in several different time points from sample rigid worms that were formed in glycerol. *Scale bar* 5 μm. **c** DSC thermogram ranging from 25 to 80°C of OCL3 polymer alone and TAX–OCL3 mixture.

RESULTS

OCL3 Filomicelles are Fluid and can Fission to Spheres

A simple physicochemical measure of aggregate stability for strongly segregating amphiphiles is the critical micelle concentration (CMC), which is expected to be exponential in the length of the hydrophobic block (36). Based on a CMC of 1.2 μg/ml for a sphere-forming OCL copolymer, EO_{44}-CL_{21} (37), we estimate an immeasurably small CMC for our OCL3 copolymer EO_{110}-CL_{58} of less than 1 fg/ml (i.e. $CMC_{OCL3} \sim [1.2\ \mu g/ml]^{58/21}$). For later comparison, Cremophor EL reportedly has a CMC_{CremEL} ~90 μg/ml. For OCL3, micellar assemblies are clearly the predominant form in any aqueous solution. Moreover, since molecular exchange rates between micelles scale inversely with CMC, these low-CMC micelles can be considered kinetically trapped or frozen—without implying glassiness or crystallinity. OCL3's weight fraction of ~0.43 for the hydrophilic PEO block drives assembly of most of the copolymer into worm-like and flexible filomicelles as observed by fluorescence microscopy after adding hydrophobic fluorescent dyes (Fig. 1b, inset). The average contour length of spontaneously assembled OCL3 filomicelles was calculated from measurement of at least 50 filomicelles, and as shown in Fig. 1b, most of the filomicelles are 6–7 μm, with some filomicelles as long as 14 μm.

Extrusion of worm-like filomicelles at high pressures and flow rates through nanoporous filters has been used to controllably reduce their length (13), but in order to convert to spherical micelles—simply and quantitatively—we exposed the filomicelles to robust sonication for several minutes. Diffusion coefficients (D_{ave}) were then measured by dynamic light scattering (DLS), and after sonication the effective hydrodynamic diameter was ~57 nm (Fig. 2). This is similar to previous ~60 nm estimates for the OCL3 filomicelle diameter of core plus corona as based on cryo-TEM (13). Prior to sonication, the measured D_{ave} proves significantly smaller and yields only a crude approximation for a larger effective size, but more important is the minimal overlap of the two distributions for D_{ave}. The 22% overlap suggests that a small fraction at most of the pre-sonicated

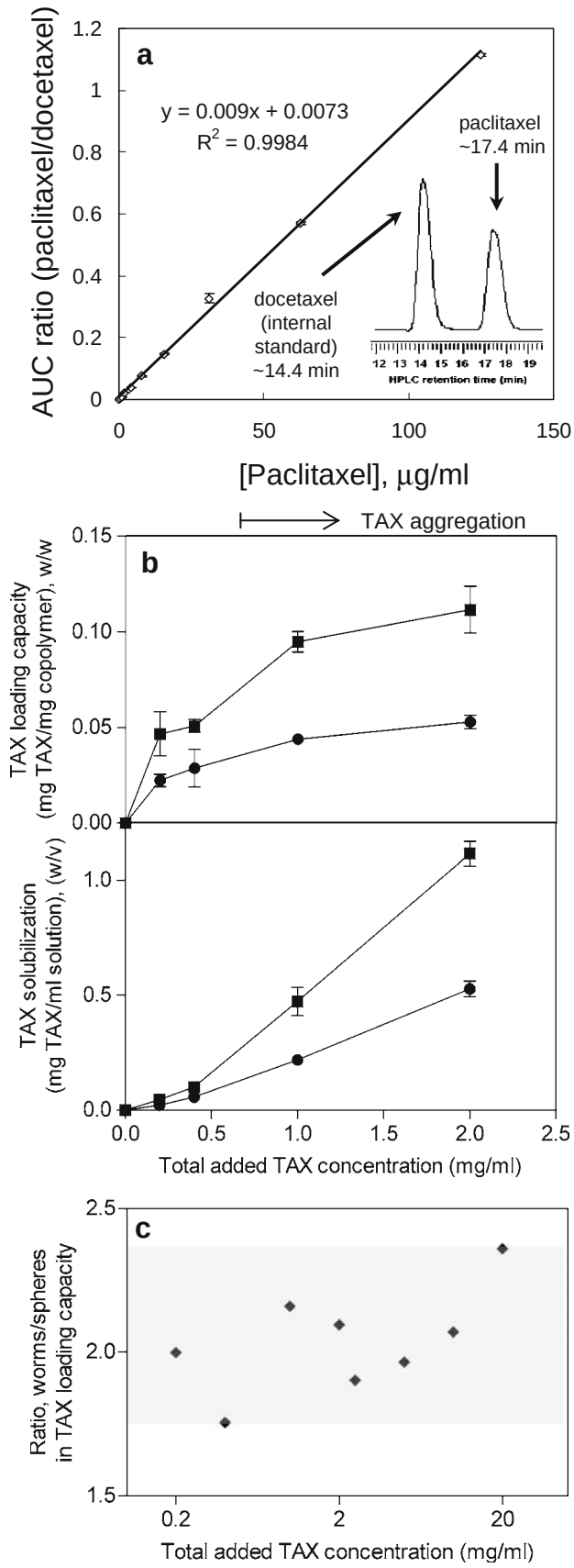

Fig. 4. HPLC-UV assay for paclitaxel (TAX) encapsulation. **a** Plot of HPLC-UV-determined area-under-curve (AUC) ratio between TAX and docetaxel vs TAX concentration. *Inset* shows the HPLC-UV spectrum of docetaxel (as internal standard) and paclitaxel (TAX). **b** TAX loading capacity (*upper panel*, defined as mg TAX loaded per milligram micelle) and solubilization (*lower panel*, defined as mg TAX loaded per milliliter aqueous solution) with OCL3 micelles when total added TAX:OCL3 micelle (*w*/*w*)=1:5; **c** ratio between TAX loading capacity with OCL3 worms and spheres at different conditions: Total added TAX:OCL3 micelle (*w*/*w*) was fixed at 1:5 while OCL3 concentration varied when added TAX concentration ≤2 mg/ml, and OCL3 micelle concentration was fixed at 10% (*w*/*v*) when added TAX concentration >2 mg/ml.

sample consists of spherical micelles. Worm-like filomicelles therefore predominate in freshly prepared OCL3 samples.

In bulk, PCL is a crystalline polymer at room temperature with melting in the range of 40–60°C (38), but past studies of PEO-based diblock copolymers in bulk suggest that PEO crystallization dominates in the same temperature range and frustrates crystallization of the connected block (38). For example, the diblock PEO-polyethylene (PE) in bulk is 70% PEO and only 10% crystalline (PE). On the other hand, dilution of filomicelles into water will generally hydrate and dissolve any crystallinity in the PEO corona. We had previously reported that OCL filomicelles appear as flexible as worm-like micelles made from non-crystalline and non-glassy diblock copolymers (e.g. PEO-polybutadiene), which implies a fluid core of PCL (30,39). However, our interest in loading and storage here involved freezing for an extended time, which are conditions that favor crystallization.

A very small fraction of the OCL3 filomicelles are inflexible coils as identified by end-to-end fluctuation<5% of the average end-to-end distances relative to the more fluid-like and flexible filomicelles (Fig. 3a). Freezing in glycerol gave up to 10% of the bent but crystalline-behaving worm-like micelles (Fig. 3a). The core fluidity of the dominant population of flexible filomicelles was subsequently estimated by fluorescence recovery after photobleaching (FRAP) studies of immobilized filomicelles (Fig. 3b). The average recovery time for four different worms was ~30 s, which is similar to that observed in PBD cores of worm-like micelles with a similar molecular weight (40). The fast recovery rate in FRAP and the minor percentage of rigid worm micelles indicate a highly fluid PCL core, which would tend to favor loading and retention of hydrophobic drugs such as paclitaxel (TAX). Fluidity also provides a basis for filomicelle flexibility, which might allow these long micelles to reptate into diseased tissues, including tumors, despite their micron-scale length.

Before examining TAX loading of filomicelles and spheres in dilute solution, we examined the bulk melting of OCL3 with or without TAX using differential scanning calorimetry (DSC). A melting onset temperature near 51°C (Fig. 3c) is consistent with PEO and/or PCL crystallization, and the finding that TAX exerted no significant effect on melting temperature indicates a relative absence of disruptive interactions between the drug and the copolymer. Assuming the melting is attributable predominantly to PEO crystallization, as cited above (41), we estimate PEO crystallinity of 81% from the measured endotherm peak area (106.3 J/g without TAX), the heat of fusion for pure PEO (~300 J/g) (41), and the f_{EO} of OCL3. With the presence of TAX, there

Table I. Validation of HPLC-UV Assay for Palictaxel, Using Docetaxel as the Internal Standard

	Values
Linear range	0.5–125 μg/ml
Intra-day CV	<15%, max 12.3%
Inter-day CV	<15%, max 14.4%
Baseline noise	~0.0001 AU
LLOD	0.5 μg/ml
LLOQ	1.0 μg/ml
Accuracy	100.2±7.8%
Recovery	101.7±6.1%

is no apparent decrease of crystalline PEO (79%) in bulk OCL3 (102.4 J/g with TAX), suggesting that TAX interaction with the copolymer is negligible.

Paclitaxel Integration into OCL3 Spheres and Filaments

TAX was then loaded into dilute micelles, and HPLC analysis was used to characterize the loading properties. An internal standard, docetaxel, was added in fixed amount to minimize variability (Fig. 4a; Table I). The lower limit of detection (LLOD) and lower limit of quantification (LLOQ) were as low as 0.5 and 1 μg/ml, and both the intra-day and inter-day coefficients of variance (CV) were less than 15%. An accuracy of 100.2 ± 7.8% (n=6) and a recovery of 101.7 ± 6.1% (n=6), were also obtained.

Loading of TAX before or after micelle formation showed no significant difference in capacity or efficiency (not shown). Figure 4b shows the TAX loading capacity and final concentration when TAX was initially added in a fixed 1:5 *w*/*w* ratio to micelles. Increasing TAX from 0.2 to 2 mg/ml (OCL3 1–10 mg/ml) increased both the loading capacity of TAX and the final solubilized TAX. Compared to spheres, OCL3 filomicelles showed about 2-fold greater loading capacity and at all concentrations (Fig. 4c).

Up to 10% *w*/*v* polymer concentration, with TAX varied from 2.5 to 5 mg/ml, the loading capacity for TAX increased, although the *w*/*w* loading was higher for 5% polymer. Further increases of added TAX up to 20 mg/ml led to a decrease in TAX solubilization regardless of morphology; this is probably due to the well-known aggregation of TAX at extremely high concentrations. The highest TAX solubilization obtained in the studies of filomicelles to date was 3 mg/ml, which is about 10,000-fold higher than natural TAX solubility in aqueous buffer [0.3 μg/ml, (18)]. Drug loading efficiency defined as (loaded drug/added drug) is tabulated in Tables II, III, and IV and consistently appears 2-fold higher with filomicelles than with spherical micelles.

Table III. Loading Efficiency of TAX into OCL3 Spherical and Worm-like Micelles at 10% (*w*/*v*) Fixed OCL3 Micelle Concentration

	Total TAX concentration (mg/ml)			
	2.5	5	10	20
Spheres	0.34	0.30	0.09	0.03
Worms	0.64	0.59	0.18	0.06

Loading Efficiency; mass of solubilized TAX/mass of initially added TAX

In addition to the encapsulation capacity studies, an identical DSC thermogram for lyophilized OCL3–TAX mixture after encapsulation (not shown) with that of OCL3–TAX mixture in bulk (Fig. 3c) again verifies the unchanged melting temperature and the fusion heat of OCL3 copolymer. This further demonstrates the absence of interactions of TAX with its excipient during the encapsulation process.

Stability and *In Vitro* Release

Possible effects of storage, drug loading and extrusion on morphological changes of filomicelles were examined by DLS and fluorescence imaging. Fig. 5a shows that (1) both shapes of micelle are morphologically stable in 4°C storage for up to 1 month; (2) TAX integration does not affect micelle size, which is probably because the small loaded mass of TAX cannot swell the relatively large cores within micelles; (3) spherical micelles made by sonicating worm-like filomicelles show no further size change after extrusion whereas filomicelles become smaller. The latter result was confirmed by contour length measurement under fluorescence microscopy (Fig. 1b), which shows that extrusion left-shifts and narrows the length distribution from 6.6–7.3 μm (95%) to 5.6–6.1 μm.

Stability of TAX loading within OCL3 micelles was evaluated after 1 month of storage. Fig. 5b shows that when TAX-loaded micelles of either morphology were either maintained in fluid form at 4°C or else frozen (and perhaps crystalline) at −20°C, no significant leakage or precipitation of TAX could be detected. As emphasized above and further below, the filomicelle carriers are clearly stable under harsh treatments. For application, freezing has the advantage in slowing hydrolytic degradation of PCL (30).

In addition, filomicelles were subjected to freeze–thaw cycles (−20°C) as another potentially disruptive operation

Table II. Loading Efficiency of TAX into OCL3 Spherical and Worm-like Micelles When Initial Added TAX:OCL3 Micelle (*w*/*w*)=1:5

	Total TAX concentration (mg/ml)				
	0.2	0.4	1	2	20
Spheres	0.11	0.14	0.22	0.26	0.03
Worms	0.23	0.25	0.47	0.56	0.06

Loading Efficiency; mass of solubilized TAX/mass of initially added TAX

Table IV. Loading Efficiency of TAX into Worm-Like OCL3 Micelles at 5 and 10% (*w*/*v*)

	Total TAX concentration (mg/ml)		
	2.5	5	10
5% Worm	0.44	0.49	0.17
10% Worm	0.64	0.59	0.18

Loading Efficiency; mass of solubilized TAX/mass of initially added TAX

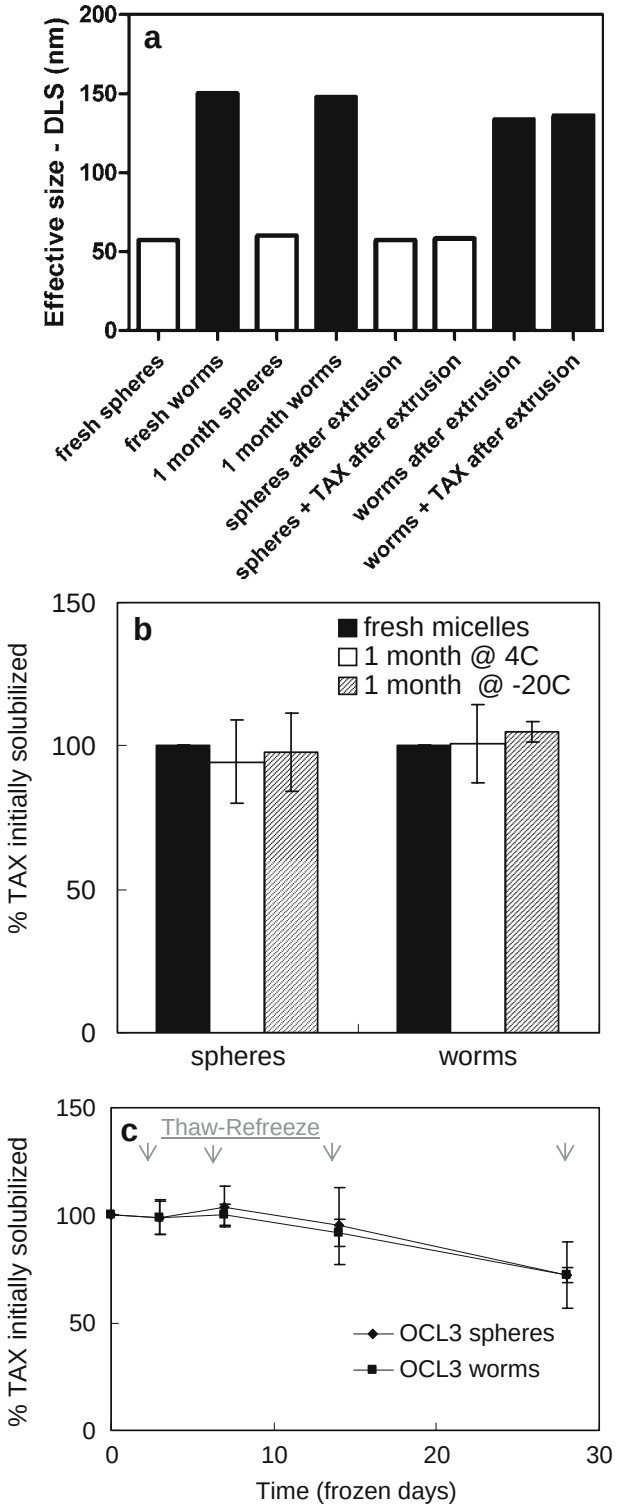

Fig. 5. Effect of extrusion, TAX loading, freeze–thawing and storage on micelle morphology and leakage of encapsulated drug. **a** Effect of extrusion, TAX loading and 1 month storage on the micelle effective size, determined by DLS; **b** effect of 1 month storage at 4 and −20°C on TAX leakage from micelles; **c** effect of multiple freeze–thawing cycles at −20°C on TAX leakage from micelles.

relevant to storage. After a single cycle, there was no significant change in the length distribution shown in Fig. 1b or in TAX retention (Fig. 5c). However, the latter plot shows that multiple freeze–thaw cycles lead to drug leakage from both morphologies. TAX-loaded OCL3 micelles were frozen at day 0, then thawed at day 3 for the test and re-frozen, which was repeated at day 7, 14, 28. By the fourth cycle, the TAX retained in the micelle cores decreased to about 70% of initial loading. The reasons are not yet as clear as the practical implications.

Release *in vitro* at 37°C was also studied at pH 7.4, per normal tissue pH, and also at pH 6.8 to mimic the slightly acidic cancerous tissue environment (29,35). As the PCL in OCL3 is known to undergo accelerated hydrolysis at acidic pH (30), TAX release rates proved to be 40% faster at lower pH but similar for both morphologies. This indicates that pH rather than shape is the more critical parameter to control drug release.

Enhanced Cytotoxicity of TAX Released from OCL3 Micelles

Human lung carcinoma-derived A549 cells were used in cytotoxicity assays of both micelles as empty carriers and also as TAX-loaded carriers. The in-clinic, commercial TAX formulation with Cremophor EL was also included as a benchmark. Excipient toxicity is critically important to assessing the specific anticancer effect of TAX, and so for ease of comparison we therefore calculate the equivalent TAX concentration; for example, 0.8 mg TAX corresponds to about 1 g Cremophor EL (see "MATERIALS AND METHODS"). Based on such analyses, Cremophor EL shows a significant cytotoxic effect at only 2–3 μg/ml equivalents of TAX (Fig. 6a). In contrast, the OCL3 polymeric micelles showed no obvious toxicity up to almost 100 μg/ml TAX equivalents. Identifying the dose of excipients at which 80% of cells are still alive ('inhibition constant' IC80) as a parameterization of toxicity and then converting to cytotoxic carrier doses yields $IC80_{CremEL}$=120 μg/ml for Cremophor EL, which appears only slightly higher than CMC_{CremEL}≈90 μg/ml and implies the aggregate form of Cremophor EL is toxic (Fig. 6b). For both filomicelles and spheres, $IC80_{OCL3\text{-}micelle}$=1,500 μg/ml, which is about 13-orders of magnitude higher than CMC_{OCL3} and suggests mechanisms of cell death such as micellar poration previously discussed for PEO-PCL polymersomes (30). Regardless, the 13-fold difference indicates, of course, that OCL3 polymeric micelles are much safer excipients.

TAX formulations with the various carriers consistently improve cytotoxicity relative to delivery of free drug. While Fig. 6c shows that TAX-loaded Cremophor EL begins killing cells in the nanogram/milliliter range of TAX and kills nearly all cells at [TAX]≅10–100 μg/ml (Fig. 6a), the Cremophor EL excipient rather than TAX is clearly responsible for a significant fraction of the cytotoxicity. On the other hand, TAX-loaded OCL3 micelles exhibit similar cytotoxicity in the 10 ng/ml range, killing more than 35% A549 cancer cells. Importantly, the anticancer effects of TAX-loaded OCL3 micelles throughout the tested concentrations were all attributed to the drug activity, instead of the toxicity from the carriers. The fitted sigmoid dose–response curve showed

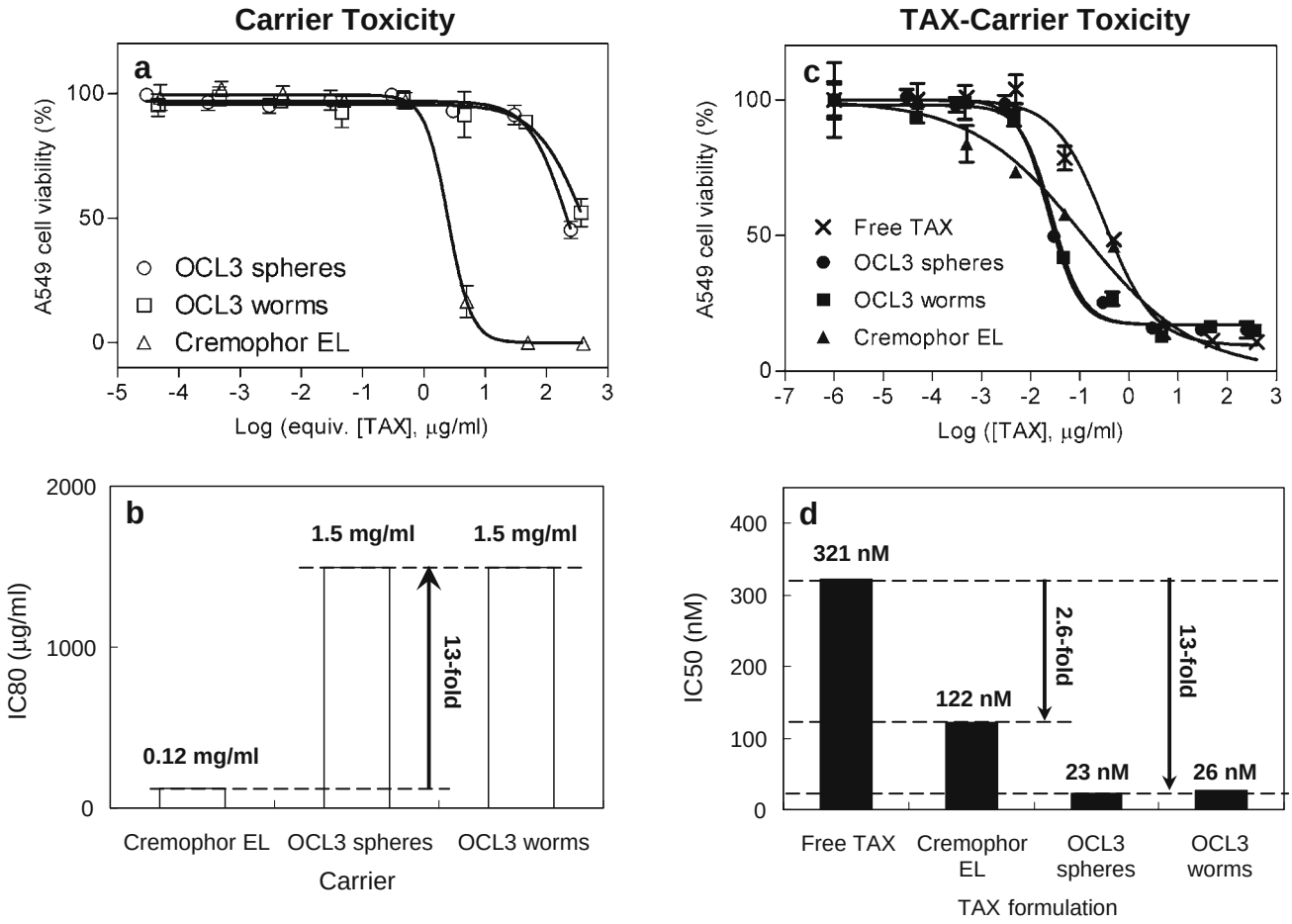

Fig. 6. Cytotoxicity study and IC50 evaluation of TAX-loaded micelles on A549 human lung carcinoma celles. **a** Cytotoxicity of excipient only (OCL3 spheres, worms, and Cremophor EL) on A549 cells; **b** comparison of the excipient concentration at which 20% cells were killed (IC_{80}); **c** cytotoxicity of different TAX formulations on A549 cells; **d** comparison of IC_{50} of different TAX formulations. Sigmoid dose–responsive equation : $Y = \text{Bottom} + (\text{Top} - \text{Bottom})/(1 + 10\text{^}((\text{Log}IC_{50} - X) * \text{HillSlope}))$, where X is the logarithm of TAX concentration, Y is the response and starts at bottom and goes to top, and HillSlope is the slope for the linear dropping region in the sigmoid curve.

that the IC50-cytotoxicity of TAX-loaded OCL3 micelles (at ~25 nM) was 13-fold more potent than free TAX (321 nM for A549 cells) and also 5-fold better than Cremophor EL TAX (Fig. 6d). Both worm-like filomicelles and spherical micelles showed the same enhanced cytotoxicity. Since OCL3 filomicelles have a higher drug loading capacity compared to spherical micelles and otherwise display similar stability and efficacy as spherical micelles, the filomicelles seem an attractive alternative for the emerging tests of parenteral delivery (13).

DISCUSSION

TAX is a widely used chemotherapeutic for cancer treatment, but its poor water solubility [0.3 μg/ml at 25°C (18)] requires clinical use of solubilizers. Cremophor EL is widely used but has side-effects and limitations that are clear both in these simple studies and in the clinic. PEO-based spherical micelles made from amphiphilic diblock copolymers have been explored as an alternative type of carrier system to load hydrophobic drugs and dyes into the hydrophobic cores, and our recent studies have focused in some detail on assembly and properties of worm-like filomicelles (30–34). The needed copolymers are typically composed of ~0.4–0.5 weight fraction of hydrophilic PEO polymer and yield flexible but highly stable filamentous micelles that surprisingly increase the circulation time in the blood stream relative to spheres. Here we showed the filomicelles -generally have a fluid core (Fig. 3), which favors integration of drugs into their hydrophobic cores, and we then examined the drug loading capacity and various other performance aspects of PEO-PCL worm-like filomicelles for comparison to spheres generated from the same filomicelles by sonication. Loading advantages are clear (Fig. 4b,c, Tables II, III, and IV), and some insight is gained from simple calculations of volume to surface area for spheres and cylinders. For spheres of radius r, volume/surface area $= (4/3\ \pi r^3)/(4\pi r^2) = r/3$, whereas for cylinders of length L, volume/surface area $= (\pi r^2 L)/(2\pi rL) = r/2$. If micellar area is thus held constant for a given mass of copolymer in solution, then the filomicelles are expected to carry more hydrophobic drug than spheres by a ratio of $(r/2 - r/3)/$

$(r/3) = 50\%$. The bigger difference of ~100% found here certainly highlights the advantageous loading of drugs into filomicelles. Furthermore, the maximum concentration of solubilized TAX reached 3 mg/ml, placing filomicelles just below Cremophor EL (marketed as formulations containing 6 mg/ml TAX) but among the top micelle-based TAX delivery systems that usually enhance TAX solubility to 1–2 mg/ml (18,21,23–25,42).

Although filomicelles appear novel and were perhaps even overlooked in past formulations that relied on sonication, PEO-PCL block copolymer has been widely explored for drug delivery applications in the past. It consists of FDA-approved PEO plus the approved and degradable polyester PCL. We have previously found that hydrolytic degradation of PCL predominates at the distal hydroxyl-end such that the hydrophobic mass of PCL gradually decreases, increasing the weight fraction of PEO and converting the worm-like micelles towards spherical micelles (30). This process is greatly accelerated by low pH, which also accelerates release of TAX. On the other hand, degradation of PCL is significantly limited at low temperatures of 4 and −20°C, and the results here demonstrate stable storage of OCL3 filomicelle morphologies at these low temperatures for a month (Fig. 5) without major complications from crystallization (Fig. 3). While multiple freeze–thaw cycles leads to loss of TAX for both worm-like and spherical micelles—as do other harsh conditions in extrusion, sonication, and lyophilization (not shown), only 1–2 cycles of freeze–thaw cycles have no obvious effect. Care should nonetheless be taken when preparing or storing TAX-loaded worm micelles.

Given the persistent circulation of filomicelles and minimal accumulation in rat lung (21), specific targeting of these novel morphologies to lung tumors should eventually provide a clear indication of directed drug delivery possibilities with filomicelles. Human lung cancer also continues to account for a significant of all cancer deaths. With these factors in mind as well as the intrinsic toxicity of Cremophor EL (Fig. 6a,b), we examined the *in vitro* delivery by filomicelles of TAX to A549 lung carcinoma cells, and we find that the spherical micelles and filomicelles are both 13-fold less toxic than Cremophor EL and, with loaded TAX, about 5-fold more effective in delivering a cytotoxic dose (Fig. 6c,d). Furthermore, since delivery of Cremophor EL is not pH-sensitive, such an *in vivo* formulation will tend to be less selective for tumors and further increase the risk of the excipient toxicity to normal cells.

CONCLUSION

Taken together, OCL3 based filomicelles appear to provide an excellent system for delivery of hydrophobic drugs, with enhanced drug solubility compared to spherical micelles but similar efficacy for a given dose of TAX. Morphological changes thus did not adversely impact drug release behavior and *in vitro* bioactivity. Future studies are likely to include conjugation with targeting moieties towards lung cancer cells and studies of *in vivo* tumor models with parenteral administration. Morphological effects under these more pathophysiological conditions clearly need to be mapped out.

ACKNOWLEDGEMENTS

This study was supported by grants from NIH-NIBIB and NSF-MRSEC.

REFERENCES

1. M. J. Vicent, R. Duncan. Polymer conjugates: nanosized medicines for treating cancer. *Trends Biotechnol.* **24**:39–47 (2006).
2. A. Malugin, P. Kopeckova, and J. Kopecek. HPMA copolymer-bound doxorubicin induces apoptosis in ovarian carcinoma cells by the disruption of mitochondrial function. *Mol. Pharmacol.* **3**:351–361 (2006).
3. Y. Luo, M. R. Ziebell, and G. D. Prestwich. A hyaluronic acid–taxol antitumor bioconjugate targeted to cancer cells. *Biomacromolecules.* **1**:208–218 (2000).
4. L. E. van Vlerkenand, and M. M. Amiji. Multi-functional polymeric nanoparticles for tumour-targeted drug delivery. *Expert Opin. Drug Deliv.* **3**:205–216 (2006).
5. B. Liu, S. Jiang, W. Zhang, F. Ye, Y. H. Wang, J. Wu, and D. Y. Zhang. Novel biodegradable HSAM nanoparticle for drug delivery. *Oncol. Rep.* **15**:957–961 (2006).
6. V. P. Torchilin. Recent advances with liposomes as pharmaceutical carriers. *Nat. Rev. Drug Discov.* **4**:145–160 (2005).
7. X. Guo, and F. C. Szoka, Jr. Chemical approaches to triggerable lipid vesicles for drug and gene delivery. *Acc. Chem. Res.* **36**:335–341 (2003).
8. F. Ahmed, R. I. Pakunlu, G. Srinivas, A. Brannan, F. Bates, M. L. Klein, T. Minko, and D. E. Discher. Shrinkage of a rapidly growing tumor by drug-loaded polymersomes: pH-triggered release through copolymer degradation. *Mol. Pharmacol.* **3**:340–350 (2006).
9. F. Ahmed, R. I. Pakunlu, A. Brannan, F. Bates, T. Minko, and D. E. Discher. Biodegradable polymersomes loaded with both paclitaxel and doxorubicin permeate and shrink tumors, inducing apoptosis in proportion to accumulated drug. *J. Control. Release.* **116**:150–158 (2006).
10. J. P. Xu, J. Ji, W. D. Chen, and J. C. Shen. Novel biomimetic polymersomes as polymer therapeutics for drug delivery. *J. Control. Release.* **107**:502–512 (2005).
11. Y. Bae, W. D. Jang, N. Nishiyama, S. Fukushima, and K. Kataoka. Multifunctional polymeric micelles with folate-mediated cancer cell targeting and pH-triggered drug releasing properties for active intracellular drug delivery. *Mol. BioSyst.* **1**:242–250 (2005).
12. J. Wang, D. Mongayt, and V. P. Torchilin. Polymeric micelles for delivery of poorly soluble drugs: preparation and anticancer activity in vitro of paclitaxel incorporated into mixed micelles based on poly(ethylene glycol)–lipid conjugate and positively charged lipids. *J. Drug Target.* **13**:73–80 (2005).
13. Y. Geng, P. Dalhaimer, S. Cai, R. Tsai, M. Tewari, T. Minko, and D. E. Discher. Shape effects of filaments versus spherical particles in flow and drug delivery. *Nat. Nanotech.* **2**:249–255 (2007).
14. X. Tong, J. Zhou, and Y. Tan. Liquid chromatography/tandem triple-quadrupole mass spectrometry for determination of paclitaxel in rat tissues. *Rapid Commun. Mass Spectrom.* **20**:1905–1912 (2006).
15. T. Y. Kim, D. W. Kim, J. Y. Chung, S. G. Shin, S. C. Kim, D. S. Heo, N. K. Kim, and Y. J. Bang. Phase I and pharmacokinetic study of Genexol-PM, a cremophor-free, polymeric micelle-formulated paclitaxel, in patients with advanced malignancies. *Clin. Cancer Res.* **10**:3708–3716 (2004).
16. S. C. Kim, J. Yu, J. W. Lee, E. S. Park, and S. C. Chi. Sensitive HPLC method for quantitation of paclitaxel (Genexol in biological samples with application to preclinical pharmacokinetics and biodistribution. *J. Pharm. Biomed. Anal.* **39**:170–176 (2005).
17. L. M. Han, J. Guo, L. J. Zhang, Q. S. Wang, and X. L. Fang. Pharmacokinetics and biodistribution of polymeric micelles of

paclitaxel with Pluronic P123. *Acta Pharmacol. Sin*. **27**:747–753 (2006).
18. O. Soga, C. F. van Nostrum, M. Fens, C. J. Rijcken, R. M. Schiffelers, G. Storm, and W. E. Hennink. Thermosensitive and biodegradable polymeric micelles for paclitaxel delivery. *J. Control. Release*. **103**:341–353 (2005).
19. R. T. Liggins, W. L. Hunter, and H. M. Burt. Solid-state characterization of paclitaxel. *J. Pharm. Sci*. **86**:1458–1463 (1997).
20. S. C. Kim, D. W. Kim, Y. H. Shim, J. S. Bang, H. S. Oh, S. Wan Kim, and M. H. Seo. In vivo evaluation of polymeric micellar paclitaxel formulation: toxicity and efficacy. *J. Control. Release*. **72**:191–202 (2001).
21. S. Cheon Lee, C. Kim, I. Chan Kwon, H. Chung, and S. Young Jeong. Polymeric micelles of poly(2-ethyl-2-oxazoline)-block-poly(epsilon-caprolactone) copolymer as a carrier for paclitaxel. *J. Control. Release*. **89**:437–446 (2003).
22. T. Meyer, D. Waidelich, and A. W. Frahm. Separation and first structure elucidation of Cremophor EL-components by hyphenated capillary electrophoresis and delayed extraction-matrix assisted laser desorption/ionization-time of flight-mass spectrometry. *Electrophoresis*. **23**:1053–1062 (2002).
23. Y. Mo, and L. Y. Lim. Preparation and in vitro anticancer activity of wheat germ agglutinin (WGA)-conjugated PLGA nanoparticles loaded with paclitaxel and isopropyl myristate. *J. Control. Release*. **107**:30–42 (2005).
24. S. Q. Liu, Y. W. Tong, and Y. Y. Yang. Thermally sensitive micelles self-assembled from poly(*N*-isopropylacrylamide-co-*N*,*N*-dimethylacrylamide)-*b*-poly(D,L-lactide-c *o*-glycolide) for controlled delivery of paclitaxel. *Mol. BioSyst*. **1**:158–165 (2005).
25. J. Xie, C. H. Wang. Self-assembled biodegradable nanoparticles developed by direct dialysis for the delivery of paclitaxel. *Pharm. Res*. **22**:2079–2090 (2005).
26. G. Gaucher, M. H. Dufresne, V. P. Sant, N. Kang, D. Maysinger, and J. C. Leroux. Block copolymer micelles: preparation, characterization and application in drug delivery. *J. Control. Release*. **109**:169–188 (2005).
27. F. Yoshii, D. Darwis, H. Mitomo, and K. Makuuchi. Cross-linking of poly(beta-caprolactone) by radiation technique and its biodegradability. *Radiat. Phys. Chem*. **57**:417–420 (2000).
28. R. T. Liggins, T. Cruz, W. Min, L. Liang, W. L. Hunter, and H. M. Burt. Intra-articular treatment of arthritis with microsphere formulations of paclitaxel: biocompatibility and efficacy determinations in rabbits. *Inflamm. Res*. **53**:363–372 (2004).
29. Z. G. Gao, D. H. Lee, D. I. Kim, and Y. H. Bae. Doxorubicin loaded pH-sensitive micelle targeting acidic extracellular pH of human ovarian A2780 tumor in mice. *J. Drug Target*. **13**:391–397 (2005).
30. Y. Geng, and D. E. Discher. Hydrolytic degradation of poly(ethylene oxide)-block-polycaprolactone worm micelles. *J. Am. Chem. Soc*. **127**:12780–12781 (2005).
31. P. Dalhaimer, F. S. Bates, and D. E. Discher. Single molecule visualization of stable, stiffness-tunable, flow-conforming worm micelles. *Macromolecules*. **36**:6873–6877 (2003).
32. Y. Kim, P. Dalhaimer, D. A. Christian, and D. E. Discher. Polymeric worm micelles as nano-carriers for drug delivery. *Nanotechnology*. **16**:S484–S491 (2005).
33. Y. Geng, F. Ahmed, N. Bhasin, and D. E. Discher. Visualizing worm micelle dynamics and phase transitions of a charged diblock copolymer in water. *J. Phys. Chem., B Condens. Mater. Surf. Interfaces Biophys*. **109**:3772–3779 (2005).
34. P. Dalhaimer, A. J. Engler, R. Parthasarathy, and D. E. Discher. Targeted worm micelles. *Biomacromolecules*. **5**:1714–1719 (2004).
35. S. D. Webb, J. A. Sherratt, and R. G. Fish. Alterations in proteolytic activity at low pH and its association with invasion: a theoretical model. *Clin. Exp. Metastasis*. **17**:397–407 (1999).
36. K. Vijayan, and D. E. Discher. Block copolymer worm micelles in dilution: mechanochemical metrics of robustness as a basis for novel linear assemblies. *J. Polym. Sci., B, Polym. Phys*. **44**:3431–3433 (2006).
37. L. Luo, J. Tam, D. Maysinger, and A. Eisenberg. Cellular internalization of poly(ethylene oxide)-*b*-poly(epsilon-caprolactone) diblock copolymer micelles. *Bioconjug. Chem*. **13**:1259–1265 (2002).
38. P. Skoglund, and A. Fransson. Continuous cooling and isothermal crystallization of polycaprolactone. *J. Appl. Polym. Sci*. **61**:2455–2465 (1996).
39. V. Balsamo, C. U. de Navarro, and G. Gil. Microphase separation vs crystallization in polystyrene-*b*-polybutadiene-*b*-poly(epsilon-caprolactone) ABC triblock copolymers. *Macromolecules* **36**:4507–4514 (2003).
40. Y. Geng, D. E. Discher, J. Justynska, and H. Schlaad. Grafting short peptides onto polybutadiene-block-poly(ethylene oxide): a platform for self-assembling hybrid amphiphiles. *Angew. Chem., Int. Ed. Engl*. **45**:7578–7581 (2006).
41. M. A. Hillmyerand, F. S. Bates. Synthesis and characterization of model polyalkane-poly(ethylene oxide) block copolymers. *Macromolecules* **29**:6994–7002 (1996).
42. J. H. Kim, K. Emoto, M. Lijima, Y. Nagasaki, T. Aoyagi, T. Okano, Y. Sakurai, and K. Kataoka. Core-stabilized polymeric micelle as potential drug carrier: increased solubilization of taxol. *Polym. Adv. Technol*. **10**:647–654 (1999).
43. G. L. Li and J. X. Tang. Diffusion of actin filaments within a thin layer between two walls. *Phys. Rev., E Stat. Nonlin. Soft Matter Phys*. **69**: Art. No. 061921 Part 1:(2004).